MINISTRY OF EDUCATION AND TRAINING

VIETNAM ACADEMY OF SCIENCE AND TECHNOLOGY

GRADUATE UNIVERSITY OF SCIENCE AND TECHNOLOGY

Trần Thị Minh

STUDY OF CHANGES IN PROLIFERATION AND CYTOSKELETAL STRUCTURE OF CHANG LIVER CELLS (CCL-13) UNDER SIMULATED MICROGRAVITY CONDITIONS

SUMMARY OF DISSERTATION ON BIOTECHNOLOGY

Code: 9420201

Hồ Chí Minh City, Year 2024

The dissertation is completed at: Graduate University of Science and Technology, Vietnam Academy Science and Technology

Supervisors:

1. Supervisor 1: PhD. Le Thanh Long, Institute of Tropical Biology, Vietnam Academy of Science and Technology

2. Supervisor 2: Professor.PhD. Hoang Nghia Son, Institute of Tropical Biology, Vietnam Academy of Science and Technology

Referee 1: Professor.PhD. Nguyen Thi Thuong Huyen

Referee 2: Professor.PhD. Nguyen Thi Thu Hoai

Referee 3: Professor.PhD. Nguyen Trong Hong Phuc

The dissertation will be examined by Examination Board of Graduate University of Science and Technology, Vietnam Academy of Science and Technology at…….. (time……, date….....)

The thesis can be accessed at:

1. Library of Graduate University of Science and Technology
2. National Library of Vietnam

INTRODUCTION

1. Rationale

The Earth gravity affects natural selection by limiting the size of an organism to an acceptable range. In order to fight gravity, living organisms would need to develop support systems such as properly supported motor structures, rigid cell membranes, and regulation of fluid flow in the body. NASA studies have shown that exposure to a microgravity environment has adverse effects on humans such as muscle atrophy and skeletal deterioration, in addition to slowing cardiovascular system function, reducing the production of red blood cells, balance disorders, vision disorders and immune system

Many devices are developed and used on Earth to simulate microgravity (SMG) conditions such as 2D-clinostat, 3D-clinostat system, and random positioning machines (RPM). The 3D rotating model (3-D clinostat) is widely used for research on zero-gravity conditions affecting different cell lines and living systems. Recent studies have shown that microgravity causes inhibition of proliferation of several cell lines such as human hematopoietic progenitor cells, bone marrow mesenchymal stem cells, and mouse mesenchymal stem cells. Furthermore, tubulin regeneration occurred in endothelial cells under microgravity. F-actin-induced reorganization inhibits migration of mouse mesenchymal stem cells induced by simulated microgravity. Simulated microgravity also affects the rat liver by altering Loureirin B metabolism and key Cytochrome P450 expression.

The liver is one of the largest organs in the human body. It plays an important role in carbohydrate, protein and lipid metabolism. Hepatocytes account for about 80% of liver volume. Up to now, there have been many studies on the activities and functions of liver cells. Most studies are usually performed on Chang hepatocytes, which are a commercially available cell line that has been shown to have biological and functional

characteristics similar to normal liver cells. However, until now there have been no specific studies on the effects of simulated microgravity on the proliferation and skeletal structure of human liver cells.

According to the request of practical need, I researched the following thesis: ***"Study of changes in proliferation and cytoskeletal structure of Chang liver cells (CCL-13) under simulated microgravity conditions***", to provide scientific evidence about the influence of simulated microgravity on the proliferation and skeletal structure changes of cells. On that basis, scientists can research further to come up with solutions to overcome the effects of microgravity on humans as well as other species.

2. The objectives of the thesis

Evaluating the effects of simulated microgravity on the proliferation and skeletonization of Chang liver cells (CCL-13) based on characteristics such as surviability, cell cycle, expression of cell cycle regulatory genes, nuclear morphological changes, apoptosis and especially the organization of microtubule and microfilament bundles by the clinostat 3-D system.

3. The main research contents of the thesis

The study focuses on evaluating the induction of Chang liver cells (CCL-13) in simulated microgravity conditions (Clinostat 3-D) with the following contents:

- Evaluation of the proliferation ability of CCL-13 cells under microgravity conditions.
- Determination of programmed death (apotosis) of CCL-13 cells under microgravity conditions.
- Evaluation of changes in CCL-13 cells cytoskeletal structure under microgravity conditions.

CHAPTER 1. LITERATURE REVIEW

1.1. Overview of microgravity

Concept of microgravity. Simulated microgravity systems such as clinostat 2-D, rotating wall vessel (RWV) system, random positioning machine (RPM), clinostat 3-D system. Research on the effects of microgravity on living systems**.**

1.2. Chang liver cell (CCL-13)

Birth of Chang hepatocytes. The "Chang Liver" cell line has been stored at ATCC (American Type Culture Collection) and is commercialized with the symbol CCL-13. Overview of current research on CCL-13 cell applications.

1.3. Overview of cell growth

Overview of cell growth, cell cycle and regulatory mechanisms. Studies on the effects of microgravity on cell growth.

1.4. Programmed cell death

Concept of programmed cell death (apoptosis). Pathways leading to cell apoptosis. Studies on the effects of microgravity on cell apoptosis.

1.5. Cytoskeleton

The structure of the cell's skeleton. Effects of microgravity environment on the formation of microtubules, microfilaments and cell division activity.

1.6. Techniques for evaluating the effects of simulated microgravity

Concepts and application principles of current techniques used to evaluate the impact of simulated microgravity conditions in cell culture such as Western Blot technique, Flow Cytometry technique, Cytell system, Immunocytochemistry (ICC) and Realtime-PCR method.

CHAPTER 2. MATERIALS AND METHODS

2.1. Materials

- Chang liver cells (CCL-13) were provided by ATCC Company.

- The clinostat 3D system creates a simulated microgravity environment designed in the project: "Research and evaluation of changes in the structure of living body cell skeleton in simulated microgravity conditions", under the Space Science and Technology Program, code: VT-CB.15/18-20.

2.2. Methods

The research contents are carried out according to the general diagram:

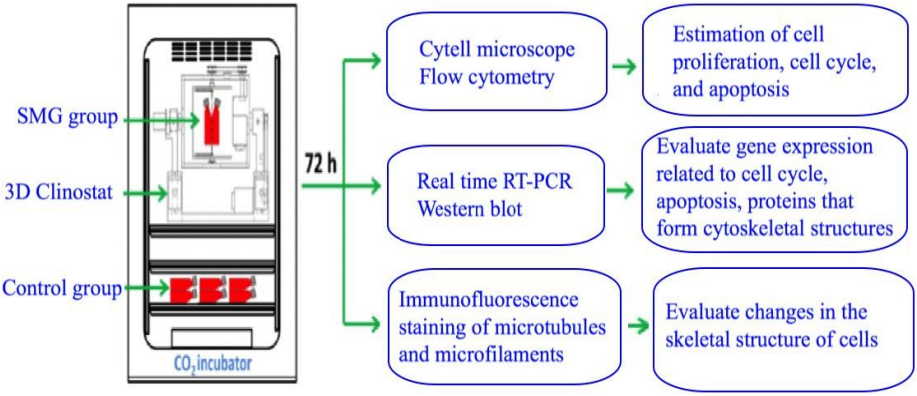

Figure 1. Schematic representation of the experimental design

2.2.1. Cell Culture

CCL-13 cells were cultured in DMEM/Ham's F-12 (DMEM-12-A, Capricorn Scientific, Ebsdorfergrund, Germany) supplemented with 15% FBS (FBS-HI-22B, Capricorn Scientific, Ebsdorfergrund, Germany) and 1% Pen/Strep (15140-122, Gibco, Thermo Fisher Scientific, Inc., Waltham, MA, USA). CCL-13 cells were divided into 2 culture groups. Simulate microgravity (SMG) group, CCL-13 cells were seeded in T-25 flasks and 96-well plates at a defined density of 1×10^5 cells/flask and 2×10^3 cells/well, respectively. Then, the T-25 flasks and 96-well plates were carefully filled with culture medium without bubbles to avoid the shearing

of fluid. The flasks and plates were mounted to the stage of inner frame of 3D clinostat (MiGra-ITB, Vietnam Academy of Science and Technology, Ha Noi, Vietnam), which was placed in a CO_2 incubator (Sanyo MCO-18AIC CO_2 Incubator, Sanyo Electric Co., Osaka, Japan) for 72 h. The control group, CCL-13 cells was treated at 1 g in the same CO_2 incubator in 72 h.

2.2.2. Cell Density Measurement by Cytell Microscope

CCL-13 cells were cultured in 96-well plates (161093, Thermo Fisher Scientific, Inc., Waltham, MA, USA) at a density of 2×10^3 cells/well for 72 h, and the cell culture was thereafter removed. The nuclei were stained with Hoechst 33342 (14533, Sigma-Aldrich, Munich, Germany) for 15 min. The cells were washed three times with phosphate-buffered saline (PBS; Gibco, Thermo Fisher Scientific, Inc., Waltham, MA, USA). The number of CCL-13 cells was determined using the Cell Cycle App. of a Cytell Microscope (GE Healthcare, Arlington Heights, IL, USA).

2.2.3. WST-1 Cell Viability Assay

CCL-13 cells were cultured in 96-well plates (161093, Thermo Fisher Scientific, Inc., Waltham, MA, USA) at a density of 2×10^3 cells/well for 72 h. Then the culture medium was removed and 100 µL fresh medium and 10 µL WST-1 (11644807001, Roche, Basel, Switzerland) were added to each well. Cells were incubated for 3.5 h at 37 °C in a 5% CO_2 atmosphere. The optical density (O.D.) was measured at 450 nm using a GloMax® Explorer Multimode Microplate Reader (Promega Corporation, Fitchburg, WI, USA).

2.2.4. Flow Cytometry Analysis

CCL-13 cells were cultured in T-25 flasks (160430, Thermo Fisher Scientific, Inc., Waltham, MA, USA) at a density of 1 × 105 cells/flask for 72 h. Flow cytometry analysis was performed using the FITC Annexin V Apoptosis Detection Kit I (556547, BD Biosciences, San Jose, CA, USA)

in BD Accuri C6 Plus (BD Biosciences, San Jose, CA, USA). To analyze cell cycle progression, CCL-13 cells were fixed with 4% paraformaldehyde (09154-85, Nacalai Tesque, Kyoto, Japan) for 15 min. CCL-13 cells were washed twice with cold PBS and resuspended in 1X Binding Buffer at a concentration of 1 × 106 cells/mL. CCL-13 cells were stained with 5 µL PI (51-66211E, BD Biosciences, San Jose, CA, USA). Cell cycle analysis was performed by measuring the cellular DNA content using a flow cytometer.

2.2.5. Evaluate nuclear morphology

CCL-13 cells were treated with 4% paraformaldehyde in PBS (Nacalai, Japan) for 30 min and were washed three times with PBS solution. We permeabilized CCL-13 cells with 0.1% Triton X-100 in PBS at 4 □ overnight. The nuclei were stained with Hoechst 33342 (14533, Sigma-Aldrich, Munich, Germany) for 15 min. The cells were washed three times with PBS (Gibco, Thermo Fisher Scientific, Inc., Waltham, MA, USA) for 10 min each. Cell cycle progression and nuclear intensity were measured with Cytell microscope (GE Healthcare, United States) using the Cell Cycle App. To evaluate the nuclear characteristics of CCL-13 cells, nuclear shape value, the parameter of Nuclear Area (µm2) was adjusted to 150 and the parameter of Sensitivity (%) was adjusted to 50 (according to the manual of the Cytell microscope).

At the same time, nuclear morphological changes of CCL-13 cells were evaluated by measuring the FSC index (Forward Scatter) using flow cytometry.

2.2.6. Quantitative real time-PCR analysis

2.2.6.1. Total RNA extraction

CCL-13 cells were lysed with trypsin-EDTA 0.25% and transferred to 1.5 ml eppendorf. Cells were lysed with 250 µl RLT solution and vortexed for 30 seconds. Add to Eppendorf 350 µl 70% Ethanol and suspend. All 700 µl sample were transferred to the RNeasy column and placed in a 2 ml

eppendorf. The sample was centrifuged at 11,000 rpm for 1 minute 30 seconds at 4^{o}C. The centrifuged fluid was discarded and 700 µl RW1 solution was added to the RNeasy column. The sample was centrifuged at 11,000 rpm for 1 minute at 4^{o}C. The centrifuged fluid was discarded and 500 µl RPE solution was added to the RNeasy column. The sample was centrifuged at 11,000 rpm for 1 minute 30 seconds at 4^{o}C. The RNeasy column is transferred to the new eppendorf. 50 µl RNase-free water was transferred to the RNeasy column. The sample was centrifuged at 11,000 rpm for 1 minute 30 seconds at 4^{o}C. The RNeasy column is removed, the total RNA sample is stored at -80^{o}C.

2.2.6.2. Real time RT-PCR performance

The expression of genes was evaluated by realtime qRT-PCR method using với kit PCRBIO 1-Step RT-PCR Kit (PCR Biosystems). Each PCR reaction contained 1 µl of template RNA, 2 µl of primers, 10µl of Mix Ro-Lox, and 1 µl of RTAse in a total volume of 20 µl. The thermal cycle were performed by: 1 cycle at 45°C for 15 minute; initial denaturation at 95°C for 2 minute; 40 cycles at 95°C for 10 seconds; 62°C for 15 seconds; and examination of the melting curve from 60°C to 95°C with 0.5 °C increases every 30 seconds. Following are the primers:

- Primer sequences for genes related to the cell cycle:

CDK4-F: 5'-ATG GAC GTC TGT GCC ACA TC-3' and CDK4-R: 5'-GTG CCT TGT CCA GAT ATG TCC-3'; CDK6-F: 5'-TCT TCA TTC ACA CCG AGT AGT GC-3' and CDK6-R: 5'-TGA GGT TAG AGC CAT CTG GAA A-3'; Cyclin A-F: 5'-GCC ATT AGT TTA CCT GGA CCC AGA-3' and Cyclin A-R: 5'-CAC TGA CAT GGA AGA CAG GAA CCT-3'; CDK2-F: 5'-CAG GAG TTA CTT CTA TGC CTG A-3' and CDK2-R: 5'-TTC ATC CAG GGG AGG TAC AAC-3'; Cyclin B1-F: 5'-AAT GAA ATT CAG GTT GTT GCA GGA G-3' and Cyclin B1-R: 5'-CAT GGC AGT GAC ACC AAC CAG-3'; Cyclin D1-F: 5'-ATG

TTC GTG GCC TCT AAG ATG A-3’ and Cyclin D1-R: 5’-CAG GTT CCA CTT GAG CTT GTT C-3’; GAPDH-F: 5’-CAT GAG AAG TAT GAC AAC AGC CT-3’ and GAPDH-R: 5’-AGT CCT TTC CAC GAT ACC AAA GT-3’.

- Primer sequences of genes related to cell apoptosis:

Bcl-2-F: 5’-TCT TCA TTC ACA CCG AGT AGT GC-3’ and Bcl-2-R: 5’-TGA GGT TAG AGC CAT CTG GAA A-3’; Bax-F: 5’-CCA GGA GTT ACT TCT ATG CCT GA-3’ and Bax-R: 5’-TTC ATC CAG GGG AGG TAC AAC-3’; GAPDH-F: 5’-CAT GAG AAG TAT GAC AAC AGC CT-3’ and GAPDH-R: 5’-AGT CCT TTC CAC GAT ACC AAA GT-3’.

- Primer sequences of genes encoding microtubules and microfilaments:

α-Tubulin 3-F: 5′-CAT TGA AAA GTT GTG GTC TGA TCA-3′ and α-Tubulin 3- R: 5′-GCT TGG GTC TGT AAC AAA GCA T-3′; β-Actin-F 5’-GAG CAC AGA GCC TCG CCT TT-3’ and β-Actin-R 5’-AGA GGC GTA CAG GGA TAG CA-3’; GAPDH-F: 5′-TTA GCA CCC CTG GCC AAG G-3’ and GAPDH-R: 5′-CTT ACT CCT TGG AGG CCA TG-3’.

2.2.7. Western Blot Analysis

Evaluation of protein expression related to cell cycle (Cyclin A1, Cyclin A2, CDK4, CDK6, CDK2, Cyclin D1), apoptosis (Bcl-2, Bax) and proteins involved in skeletal structure of cells (α-tubulin 3, β-actin) by Western Blot method. At the same time, GAPDH protein was used as a control. Steps include: protein lysis, SDS-PAGE electrophoresis, transfer to PVDF membrane, membrane blocking, primary antibody incubation, secondary antibody incubation, and X-ray film development.

CCL-13 cells were harvested from T-25 flasks, and the lysate was prepared with Optiblot LDS Sample Buffer (ab119196, Abcam, Cambridge, MA, USA). Equal amounts of protein (10 μg/well) were loaded into the wells of the Precast Gel SDS-PAGE 4–12% (ab139596, Abcam,

Cambridge, MA, USA). The gel was run in Optiblot SDS Run Buffer (ab119197, Abcam, Cambridge, MA, USA) for 2 h at 50 V. The protein was transferred to a PVDF membrane (ab133411, Abcam, Cambridge, MA, USA), and the membrane was blocked overnight at $4^{O}C$ with blocking buffer (ab126587, Abcam, Cambridge, MA, USA). The membrane was incubated with primary antibodies in blocking buffer overnight at $4^{O}C$. Anti-Cyclin A1 + Cyclin A2 antibody (ab185619, Abcam, Mỹ), Anti-Cdk4 antibody (ab137675, Abcam, Mỹ), Anti-Cyclin D1 antibody (ab40754, Abcam, Cambridge, MA, Mỹ), Anti-Cdk6 antibody (ab124821, Abcam, Mỹ), Anti-Bax antibody (ab53154, Abcam, Cambridge, MA, Mỹ) and Anti-Bcl-2 antibody (ab196495, Abcam, Cambridge, MA, Mỹ) were employed at the 1:5000 dilution. Anti- β-Actin antibody (ab8226, Abcam, Mỹ) and Anti-α-Tubulin 3 antibody (ab52866, Abcam, Mỹ) were employed at the 1:10000 dilution. Anti-GAPDH (ab181602, Abcam, Cambridge, MA, USA) was used as the control, at a 1:10000 dilution. The membrane was washed three times with TBST for 10 min each. The membrane was incubated with secondary antibody in blocking buffer at room temperature for 1 h. The blots were visualized using the ECL Western Blotting Substrate Kit (ab65623, Abcam, Cambridge, MA, USA). Imaging was carried out with an X-ray film.

2.2.8. Microtubule Staining

CCL-13 cells were cultured in 96-well plates at a density of 2×10^3 cells/well, in 395 µL/well culture medium. Microtubules were stained 2 µl SiR-Tubulin (CY-SC002, Cytoskeleton, Inc., Denver, CO, USA) with 50 nM SiR-tubulin/well. The structure of microtubule bundles was evaluated under a Cytell microscope (GE Healthcare, Chicago, IL, USA).

2.2.9. Microfilament Staining

CCL-13 cells were cultured in 96-well plates at a density of 2×10^3 cells/well. CCL-13 cells were fixed with 4% paraformaldehyde (Nacalai

Tesque, Kyoto, Japan) for 30 min, before being permeabilized with 0.1% Triton X-100 (Merck, Darmstadt, Germany) overnight at 4 °C. Phalloidin CruzFluorTM 488 Conjugate (sc-363791, Santa Cruz Biotechnology, Santa Cruz, CA, USA) was used to stain actin filaments for 1 h. The structure of the microfilament bundles was evaluated under a Cytell microscope (GE Healthcare, Chicago, IL, USA).

2.2.10. Statistical Analysis

The data were analyzed using Sigma Plot software (SYSTAT Software, USA). One-way ANOVA method was used to evaluate differences between experimental groups, where $p \leq 0.05$ was considered statistically significant.

Chapter 3. RESULTS AND DISCUSSION

3.1. Proliferation of Chang Liver Cells under SMG

3.1.1. Changes in CCL-13 cell density under SMG

The number of CCL-13 cells was counted using the Cell Cycle App. of a Cytell Microscope. The analysis results in Figure 3.1A show that the number of CCL-13 cells in the SMG group (7092 ± 432 cells/well) was lower than that of the control group (10101 ± 171 cells/well) over the 3-day culture ($p \leq 0{,}005$).

The WST-1 assay was also employed to assess CCL-13 cell proliferation. The absorbance value of CCL-13 cells in the control group in the 3-day culture was 0.76 ± 0.01, which was higher than that of cells in the SMG group (0.62 ± 0.03) (Figure 3.1B). These results indicated that CCL-13 cells from the SMG group exhibited lower proliferation than cells from the control group.

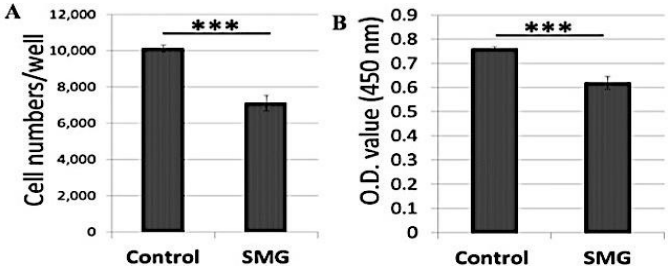

Figure 3.1. Proliferation of CCL-13 cells in control and SMG groups (n=12). (A) The number of cells was counted using the Cytell microscope. (B) Cell proliferation was assessed by WST-1 assay. ***$p < 0.001$

The CCL-13 cells in the SMG group had a larger area than the cells in the control group (1209.00 ± 81.12 μm^2 vs. 1000.42 ± 56.14 μm^2, respectively) (Figure 3.2). These results show that under SMG conditions the proliferation ability of CCL-13 cells is reduced. At the same time, the CCL-13 cell area in SMG condition was large compared to the control group.

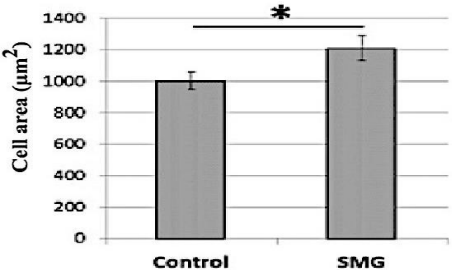

Figure 3.2. CCL-13 cells area under two culture conditions. * $p < 0.05$

3.1.2. Effect of SMG on CCL-13 cells cycle

3.1.2.1. Result of flow cytometry analysis

The cycle progression of CCL-13 cells was evaluated by flow cytometry. The ratio of SMG cells in the G0/G1 phase was higher than the control cells (90.60 ± 0.40% vs. 86.93 ± 0.23%, respectively) (Figure 3.3). The percentage of CCL-13 cells in the S phase and G2/M phase was higher in the control cells than the SMG cells. These data revealed that SMG conditions resulted in CCL-13 cells moving to the cell cycle arrest phase.

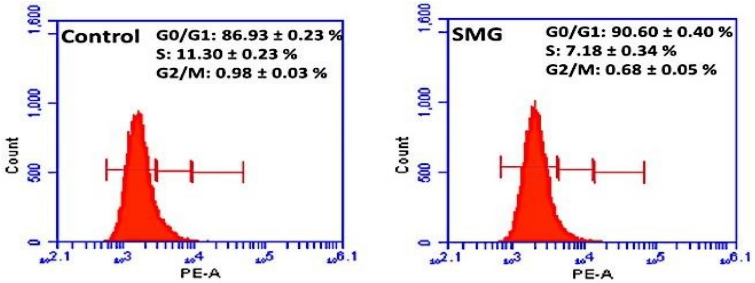

Figure 3.3. CCL-13 cells cycle was analyzed by flow cytometry (n = 12)

3.1.2.2. Transcriptional expression of cell cycle regulatory genes

Realtime PCR analysis results showed that the CCL-13 cells in the SMG group had reduced mRNA expression of Cyclin A (Figure 3.4A), Cyclin D (Figure 3.4B) and CDK6 genes (Figure 3.4D). However, CDK4 gene mRNA expression had no statistical difference between the two experimental groups (Figure 3.4C).

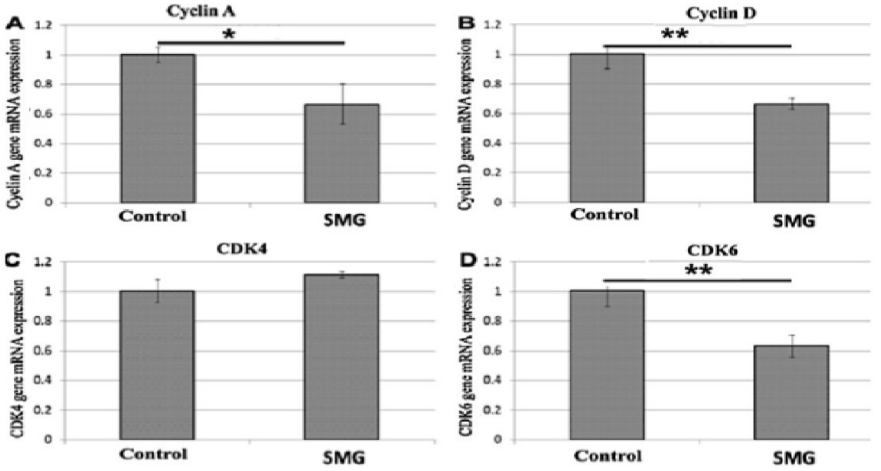

Figure 3.4. Realtime RT-PCR analysis of cell cycle regulatory genes

Compared with the cells of the control group, CCL-13 cells of the SMG group had reduced transcriptional expression levels of the Cyclin B1 and Cyclin D1 genes (Figure 3.5). The expression of Cyclin B1 and Cyclin D1 genes of CCL-13 cells treated with SMG was lower than that of the control group. At the same time, the transcriptional expression of CDK2 and CDK6 genes in the SMG group was also lower than the control group. These results showed that under SMG conditions there was reduced transcriptional expression of CCL-13 cell cycle regulatory genes.

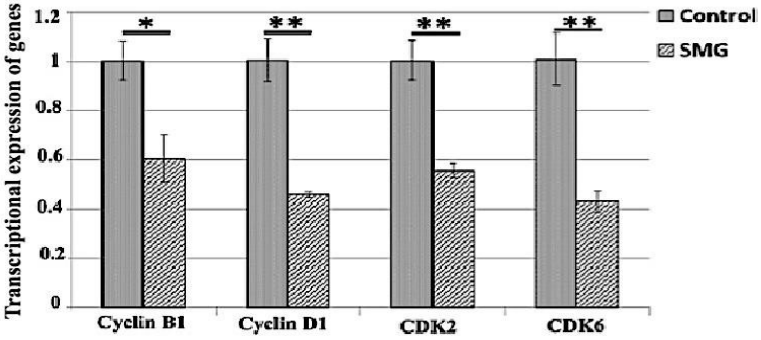

Figure 3.5. Comparison of transcriptional expression of cell cycle-related genes in the SMG group and the control group. ** $p < 0.01$; * $p < 0.05$

3.1.2.3. Translational expression of cell cycle regulatory genes

Figure 3.5 showed that the CCL-13 cells from the control group had a higher expression of Cyclin A1+A2, Cyclin D1, and CDK 6 proteins than cells in the SMG group. However, there was no difference in CDK4 expression between the control and SMG cells (Figure 3.6).

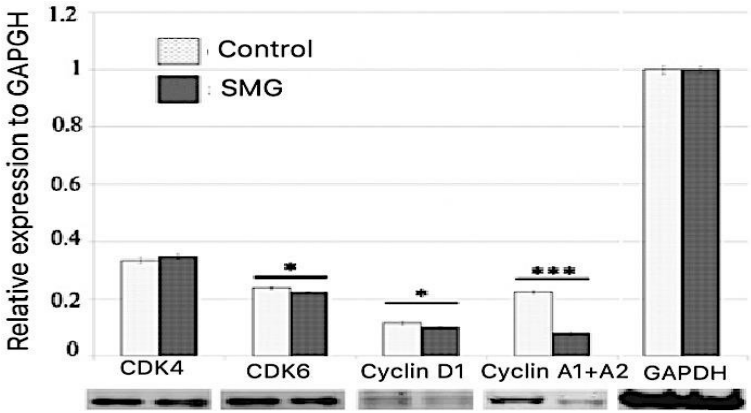

Figure 3.6. Western blot analysis of CCL-13 cell cycle regulatory proteins (n = 3). *** $p < 0.001$; ** $p < 0.01$; * $p < 0.05$

3.2. Effect of SMG on CCL-13 cell apoptosis

3.2.1. Changes in nuclear shape and nuclear intensity of CCL-13 cells

The nuclei of CCL-13 cells in the control and SMG group both had normal morphology, without chromatin condensation or nuclear fragmentation (Figure 3.7). This shows that apoptosis does not occur in the analyzed cells.

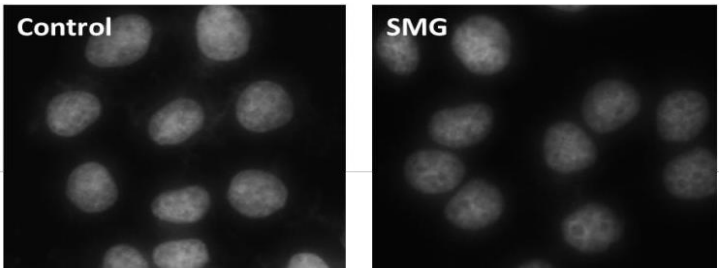

Figure 3.7. Nuclear morphology of CCL-13 cells

The effects of SMG on CCL-13 cell proliferation were further estimated by morpholog- ical evaluation. The FSC value of CCL-13 cells in the SMG group was higher than that of cells in the control group (9.80×10^6 vs. 8.78×10^6, respectively) ($p < 0.001$) (Figure 3.8A), suggesting that the diameter of CCL-13 cells in the SMG group was greater than that of cells in the control group. This result is consistent with the results in Figure 3.2 in terms of cell area. The nuclear area of CCL-13 cells in the SMG group was lower than that of cells in the control group (244.50 ± 2.79 μm^2 vs. 254.75 ± 1.41 μm^2, respectively) ($p < 0.01$) (Figure 3.8B). The parameter of nuclear generated by the Cytell microscope is nuclear form factor (1.0 = circle, <1.0 = non-circular), which evaluates nuclear integrity; there was no difference in the nuclear form factor in CCL-13 cells in both groups (Figure 3.8C). This proves that SMG condition does not affect the nuclear shape value nor the nuclear integrity of CCL-13 cell.

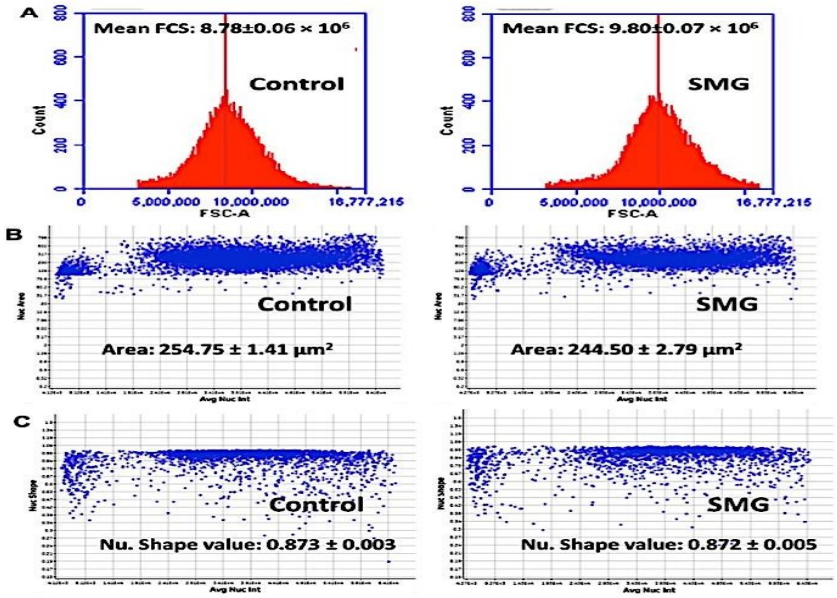

Figure 3.8. Morphology of CCL-13 cells. **A**: The mean forward scatter (FSC), **B**: The nuclear area, **C**: The nuclear shape value

The nuclear area of CCL-13 cells in the SMG group (244.45 ± 3.80 μm^2) was smaller than that of the control group (254.75 ± 2.95 μm^2) (Figure 3.9A). This decreased the nuclear/cytoplasmic ratio of CCL-13 cells under the SMG group (23.29 ± 1.46%) compared with the control group (29.15 ± 1.80%) (Figure 3.9 B)

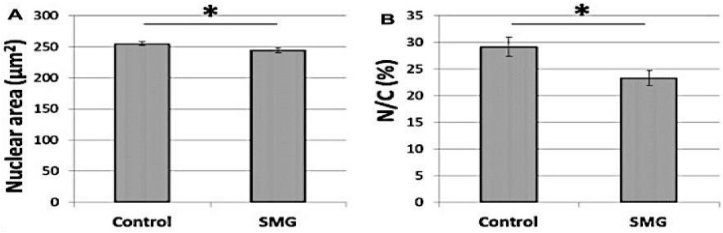

Figure 3.9. The nuclear area (A) and the nuclear/cytoplasmic ratio of CCL-13 cells (B). * p <0,05

Figure 3.10A and figure 3.10B show that under SMG conditions, CCL-13 cells have lower nuclear intensity than the control group (37766 ± 458 vs. 39985 ± 366, respectively). The result was less chromatin condensation that reduced the division of CCL-13 cells.

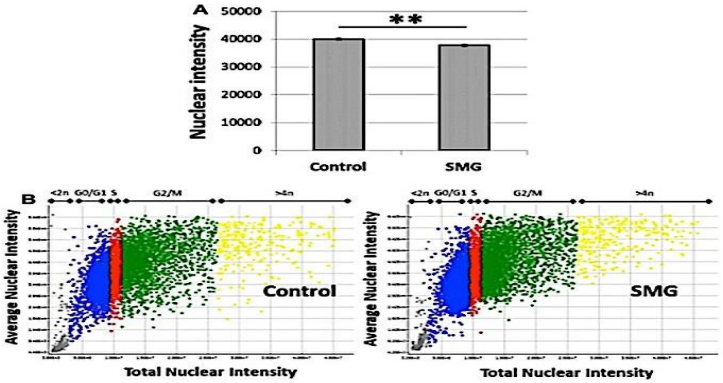

Figure 3.10. Nuclear intensity (A); Distribution of CCL-13 nuclear intensity (B). Gray represents the percentage of nuclei < 2n, blue is the percentage of nuclei in G0/G1 phase, red is the percentage of nuclei in S phase, green represents the percentage of nuclei in G2/M phase, and yellow represents the percentage of nuclei >4n. ** p < 0.01

3.2.2. Effect of SMG on apoptosis of CCL-13 cells

3.2.2.1. Percentage of CCL-13 cells entering the apoptosis pathway

Flow cytometry analysis demonstrated that CCL-13 cells in both groups exhibited similar percentages of viability (98,83 ± 0,05 % vs. 99,07 ± 0,05 %, respectively). (Figure 3.11). However, there was no statistical difference in the percentage of cell viability between these two groups. This shows that SMG conditions do not affect the vitality of CCL-13 cells. In addition, analysis results showed that the rate of CCL-13 cells with apoptosis in the control group was 0.73 ± 0.05%, higher than in the SMG group, 0.70 ± 0.07%. However, there was no statistical difference in the rate of cell apoptosis between these two groups. This shows that SMG condition does not affect the apoptosis of CCL-13 cells.

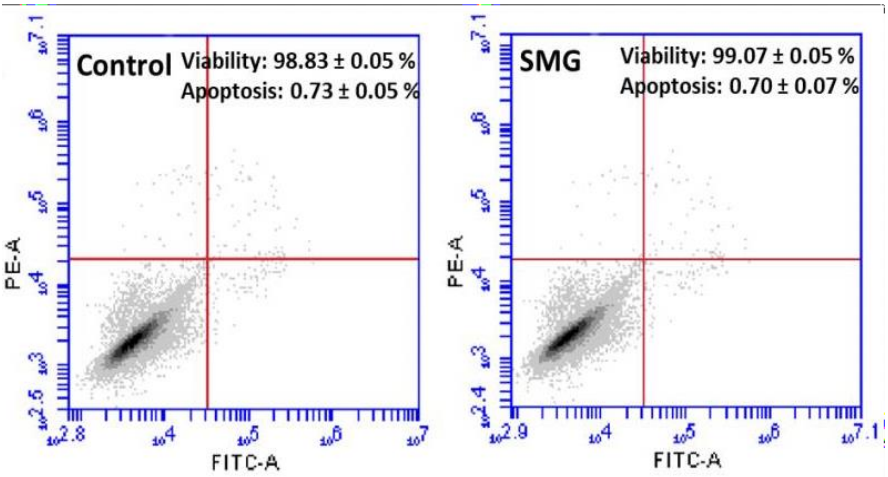

Figure 3.11. The apoptosis and viability of CCL-13. (A) Flow cytometry analysis of apoptosis viability in CCL-13 cells (n=4)

3.2.2.2. Transcript expression of genes related to apoptosis

Bcl-2 and Bax genes have an important role in balancing the rate of cell apoptosis. Realtime RT-PCR analysis results showed that there was no difference in the expression of Bax gene and Bcl-2 gene at the transcription

level of CCL-13 cells between the two control groups and the SMG group. (Figure 3.12).

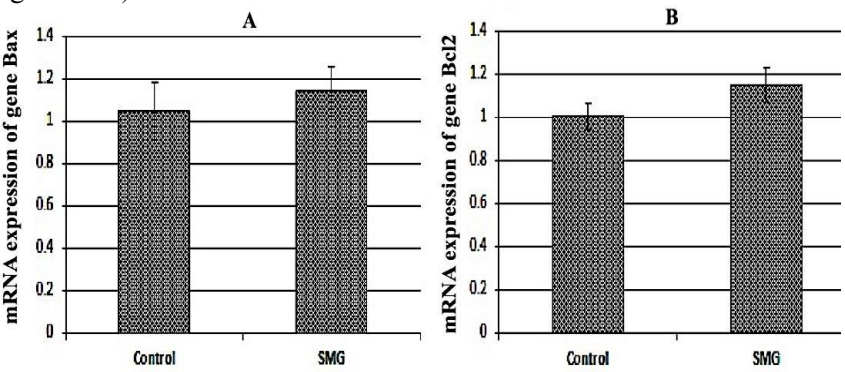

Figure 3.12. Bax gene (A) and Bcl2 gene (B) mRNA expression

3.2.2.3. Expression of translation levels of Bcl-2 and Bax genes

Figure 3.13 shows that there is no difference in Bcl-2 and Bax protein expression of CCL-13 cells between the control and SMG groups.

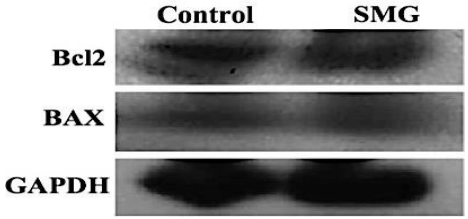

Figure 3.13. Analysis results of Bax and Bcl-2 protein expression

3.3. Changes in CCL-13 cytoskeletal structure under SMG conditions

3.3.1. Expression of genes related to cytoskeletal structures

3.3.1.1. Transcript expression of α-tubulin 3 gene and β-actin gene

In SMG conditions, CCL-13 cells reduced α-Tubulin 3 gene expression by 18% compared to the control group (Figure 3.14A). At the same time, β-Actin gene expression under SMG conditions of CCL-13 cells was strongly reduced by up to 80% (Figure 3.14B). This shows that SMG conditions reduce α-Tubulin 3 and β-Actin genes expression at the transcription level and significantly change the CLL-13 cell cytoskeletal structure.

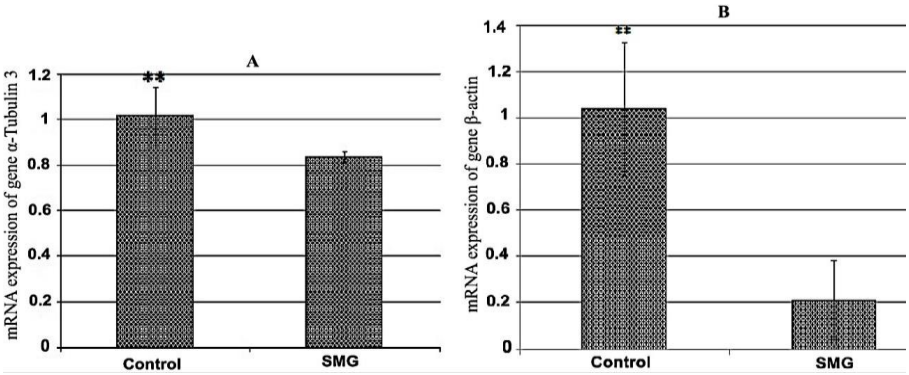

Figure 3.14. α-Tubulin 3 (A) and β-actin (B) genes mRNA expression. **P<0.001

3.3.1.2. Effects of SMG on Cytoskeletal Protein Expression

In SMG conditions, CCL-13 cells had a greater decrease in expression of β-Actin and α-Tubulin 3 proteins compared to the control group (Figure 3.15). This result further strengthens the results of Realtime RT-PCR analysis. Expression of α-Tubulin 3 and β-Actin genes in CCL-13 cells decreased at both the transcriptional and translational levels under SMG conditions. This affects the composition and content of tubulin and actin, thereby changing the structure of microtubules and microfibers as well as the distribution of microtubules and microfibers in CCL-13 cells.

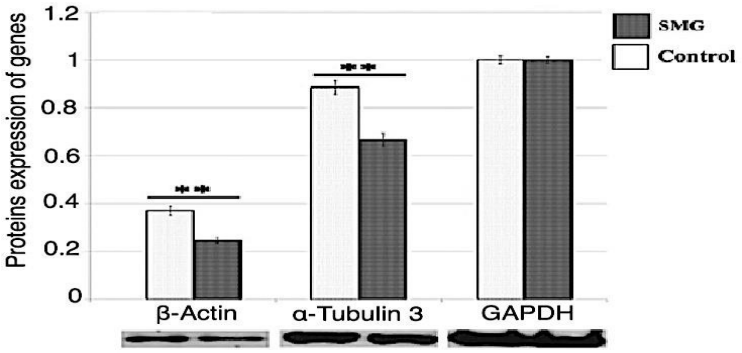

Figure 3.15. Expression of α –Tubulin and β-actin proteins. **P<0.001

3.3.2. Changes in CCL-13 cell cytoskeletal structure

3.3.2.1. Changes in microtubule structure of CCL-13 cells

Figure 3.16 shows that microtubules in the control group are more densely distributed than in the SMG group. CCL-13 cells in the control group had a morphology similar to liver epithelial cells and their microtubule bundles were distributed parallel along the length of the cell. This distribution was not observed in cells in the SMG group, instead there was an interwoven distribution of microtubule bundles in the cytoplasm. Tubulin protein staining results showed that under SMG conditions, CCL-13 cells expanded into a circular shape instead of elongating. In addition, the microtubule bundles were concentratedly distributed in the nucleus in CCL-13 cells in the control group, whereas the microtubule system was evenly distributed in CCL-13 cells in the SMG group.

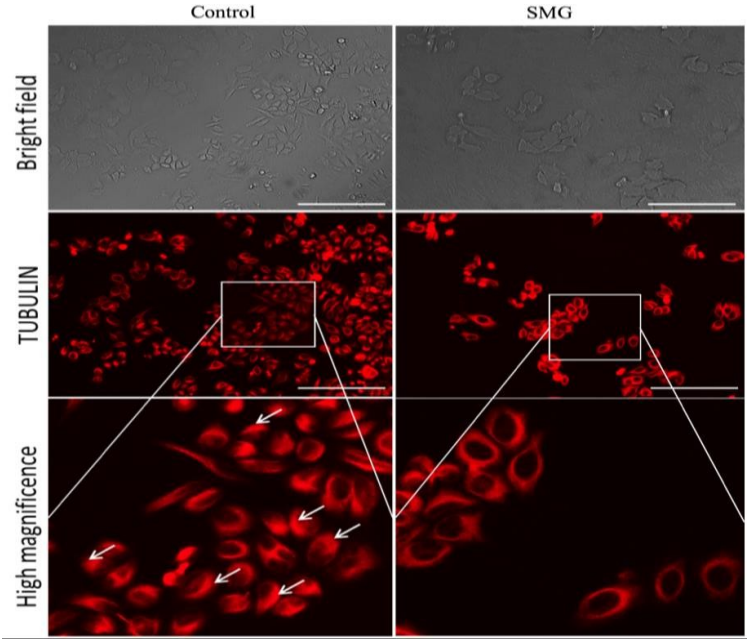

Figure 3.16. Results of Tubulin protein staining that forms microtubules bundles of CCL-13 cells, Scale bar = 223.64 µm

3.3.2.2. Changes in microfilament structure of CCL-13 cells

The results of actin microfilament staining in Figure 3.17 show that CCL-13 cells in the control group have a parallel distribution of microfiber bundles and extend across the cell length. In the SMG group, actin microfilaments displayed lower density. The results showed that CCL-13 cells under SMG conditions tended to expand into a round shape instead of elongating.

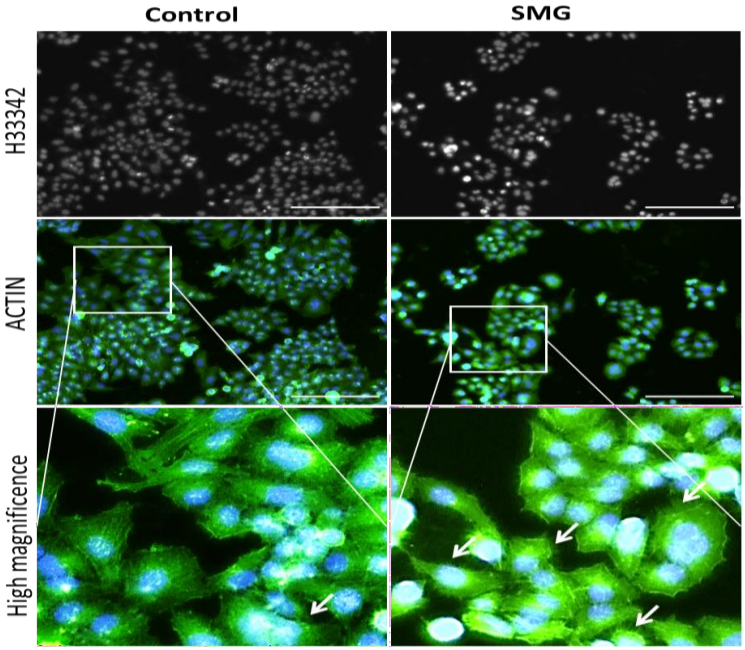

Figure 3.17. Results of Actin protein staining that forms microfilaments bundles of CCL-13 cells, Scale bar = 223.64 µm

3.3.2.3. Effects of SMG on morphological changes during cell division

Microfilament and microtubule staining were applied to assess the effects of SMG condition on two structures related to cell division, including the contractile ring and spindle. As shown in Figure 3.18a, CCL-13 cells from the control group rounded up with apical shape during mitosis and exposed the abundant appearance of microvilli. In the last step of cell

division, CCL-13 cells exhibited contractile ring formation, which generates the constricting force to separate one cell into two sister cells (Figure 3.18b). The microvilli appearance was also detected in CCL-13 cells from SMG group in mitosis (Figure 3.18c) as well as the contractile ring formation in these cells during cytokinesis (Figure 3.18d). However, the SMG treated CCL-13 cells showed a lower intensity of microfilament in these structures, compared to the control cells. The CCL-13 cells from both groups showed similar normal morphology without fragmentation and condensation which are the characteristics of apoptosis.

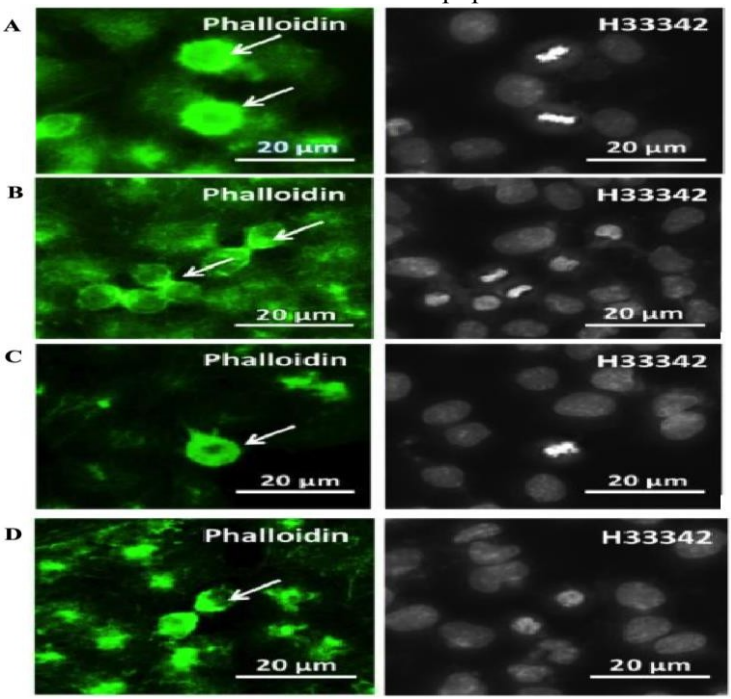

Figure 3.18. Microfilament staining of CCL-13 cells: (a,b) The appearance of contractile ring and microvilli in the control CCL-13 cells; (c,d) The appearance of contractile ring and microvilli in CCL-13 cells under SMG condition. Microfilaments and nuclei were counterstained with Phalloidin (green) and H33342, respectively.

The microtubule staining indicated that CCL-13 cells in the control group and SMG group showed ormal spindle formation during mitosis (Figure 3.19a-c, Figure 3.19g-i). During cytokinesis, the control CCL-13 cells displayed the normal structure of polar spindle microtubules (Figure 3.19d-f) while the irregular form of this structure was discovered in SMG CCL-13 cells (Figure 3.19k-m). This result showed that SMG affected the structure formation of polar spindle microtubules during sister cell separation.

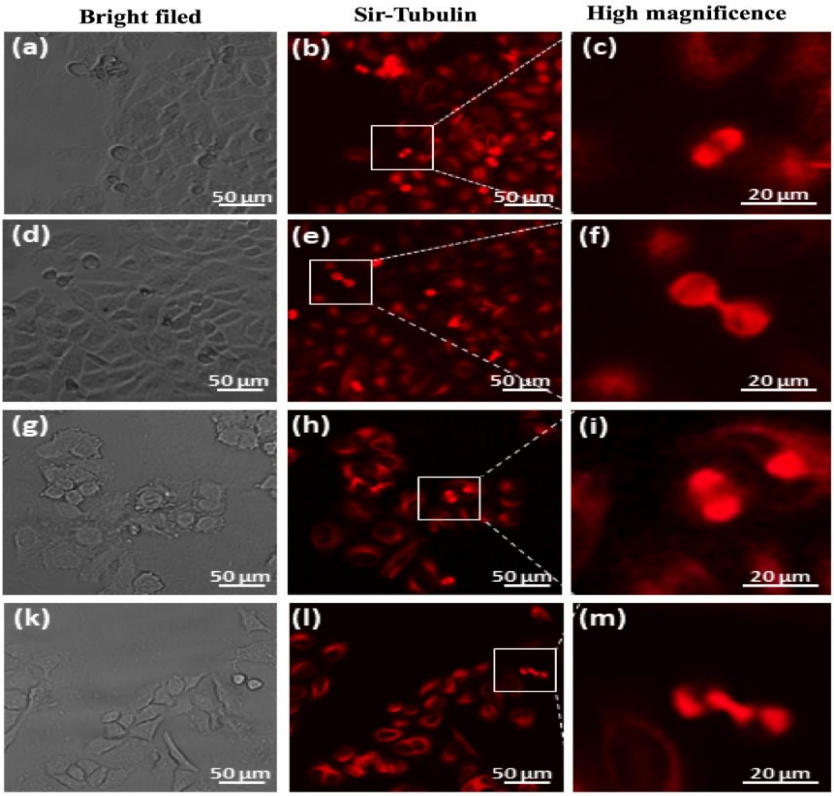

Figure 3.19. Microtubule staining of CCL-13 cells: (a-c and d-f) The appearance of the spindle in the control CCL-13 cells; (g-i and k-m) The appearance of the spindle in the CCL-13 cells in SMG group.

CONCLUSION AND RECOMMENDATION

Conclusion

The results showed that The CCL-13 cells from the control group and the SMG group exhibited the typical epithelial-like shape. SMG reduced CCL-13 cell proliferation by an increase in the number of CCL-13 cells in G0/G1 phase. This cell cycle phase arrest of CCL-13 cells was due to a downregulation of cell cycle-related proteins, such as Cyclin A, Cyclin B1, Cyclin D1, and cyclin-dependent kinase (Cdk2 and Cdk6). The changes in the cell cycle of CCL-13 cells were impacted by SMG condition, which was shown in the rise of cell percentage in G0/G1 phase and the decrease in S phase and G2/M phase. Moreover, the transcript expression of cyclin b1, cyclin d1, cdk2, and cdk6 was down-regulated in CCL-13 cells under SMG condition compared to the control group.

The CCL-13 cells of both groups displayed normal nuclear morphology and were devoided of the fragmentation and condensation. The cell area of SMG-exposed CCl-13 cells was increased while their nuclear area was decreased. The apoptosis rate of CCL-13 cells between the two experimental groups was similar and there was no statistical difference. At the same time, the expression of Bcl-2 and Bax genes also had no statistical difference in both the SMG group and the control group.

SMG-exposed CCL-13 cells also exhibited a downregulation of α-tubulin 3 and β-actin which induced the cytoskeleton reorganization. Interestingly, SMG-exposed CCL-13 cells exhibited the low appearance of microvilli, the changes in the formation of the contractile ring, and polar spindle microtubules during cytokinesis.

Recommendation

Research needs to be carried out on more cell lines and tested with more time points to clarify the mechanism of impact of simulated microgravity conditions on cell growth.

LIST OF THE PUBLICATIONS RELATED TO THE DISSERTATION

1. Chi Nguyen Quynh Ho [1,2,†] , **Minh Thi Tran [2,3,†]**, Chung Chinh Doan [1,2], Son Nghia Hoang [1,2], Diem Hong Tran [4] and Long Thanh Le [1,2,*]. Simulated Microgravity Inhibits the Proliferation of Chang Liver Cells by Attenuation of the Major Cell Cycle Regulators and Cytoskeletal Proteins. *Int. J. Mol. Sci.* 2021, *22*, 4550. https://doi.org/10.3390/ijms22094550.

2. **Minh Thi Tran [1,2]**, Chung Chinh Doan [2,3], Son Nghia Hoang [2,3], Cang Ngoc Ly [3], Mai Thi Phuong Nguyen [4], Quan Minh To[5], Nhung Hai Truong[5], Chi Nguyen Quynh Ho [2,3,*] and Long Thanh Le [2,3,*]. The changes in the cell division of Chang liver cells induced by simulated microgravity. *Appl. Sci.* 2023, *13*, x. https://doi.org/10.3390/xxxxx.